Substrate polypeptide presents a load on the apical domains of the chaperonin GroEL

Fumihiro Motojima*†‡, Charu Chaudhry§¶, Wayne A. Fenton*, George W. Farr*†, and Arthur L. Horwich*†‖

*Department of Genetics and †Howard Hughes Medical Institute, Yale School of Medicine, Boyer Center, New Haven, CT 06510; and §Department of Molecular Biophysics and Biochemistry, Yale University, New Haven, CT 06512

This contribution is part of a special series of Inaugural Articles by members of the National Academy of Sciences elected on April 29, 2003.

Contributed by Arthur L. Horwich, August 19, 2004

A conundrum has arisen in the study of the structural states of the GroEL–GroES chaperonin machine: When either ATP or ADP is added along with GroES to GroEL, the same asymmetric complex, with one ring in a GroES-domed state, is observed by either x-ray crystallographic study or cryoelectron microscopy. Yet only ATP/GroES can trigger productive folding inside the GroES-encapsulated cis cavity by ejecting bound polypeptide from hydrophobic apical binding sites during attendant rigid body elevation and twisting of these domains. Here, we show that this difference occurs because polypeptide substrate in fact presents a load on the apical domains, and, although ATP can counter this load effectively, ADP cannot. We monitored apical domain movement in real time by fluorescence resonance energy transfer (FRET) between a fixed equatorial fluorophore and one attached to the mobile apical domain. In the absence of bound polypeptide, addition of either ATP/GroES or ADP/GroES to GroEL produced the same rapid rate and extent of decrease of FRET ($t_{1/2}$ < 1 sec), reflecting similarly rapid apical movement to the same end-state and explaining the results of the structural studies, which were all carried out in the absence of substrate polypeptide. But in the presence of bound malate dehydrogenase or rhodanese, whereas similar rapid and extensive FRET changes were observed with ATP/GroES, the rate of FRET change with ADP/GroES was slowed by >100-fold and the extent of change was reduced, indicating that the apical domains opened in a slow and partial fashion. These results indicate that the free energy of γ-phosphate binding, measured earlier as 43 kcal per mol (1 cal = 4.184 J) of rings, is required for driving the forceful excursion or ''power stroke'' of the apical domains needed to trigger release of the polypeptide load into the central cavity.

Chaperonins are large ring assemblies that play an essential role in the cell in the final step of information transfer from DNA to effector protein: They assist polypeptide chain folding to the native state through the consumption of ATP. Although the early studies of Anfinsen (1) showed that polypeptide chains contain sufficient information in their primary structure to direct folding to the native state, typically the thermodynamic minimum, polypeptides can misfold during this process under cellular conditions of high temperature and solute concentration, and thus the cell has evolved components that provide kinetic assistance to enable rapid and efficient attainment of the native state (2–4). These specialized proteins, known as molecular chaperones, act in general by recognizing nonnative substrate proteins through their selective exposure of hydrophobic surfaces, surfaces that are typically buried in the interior of a protein in its native state.

Chaperones, through their own hydrophobic binding sites, bind nonnative states in a variety of different topologic contexts, e.g., as extended segments (Hsp70 family) or in collapsed forms (Hsp60 family), serving to stabilize nonnative forms or even reverse their incipient misfolding. Subsequently, in many cases through the action of binding ATP, chaperones change their own conformations such that they release polypeptide substrates, allowing them, for example, to pursue a trial of folding to native form or to pass through a translocon. In many cases, multiple cycles of such binding and release, essentially a trial and error process, are required for a productive outcome. In the cellular context, such cycles within any given compartment involve a partitioning of released protein substrate between a network of different chaperones such that, depending on the binding kinetics, the substrate can be directed to a fate ranging from folding to native form, at one extreme, to unfolding and degradation by the proteolytic system, at the other.

The chaperonin class (Hsp60) of double-ring chaperones appears to be unique in ability to promote the native state inside the central cavity of a ring (5–8). Chaperonins accomplish such action through both a step of binding a nonnative substrate protein in an open ring (9–11), serving to prevent it from misfolding and aggregation and perhaps unfolding it further, and a subsequent step of folding, carried out after release into a now encapsulated central cavity (5–8, 12) that has an altered character of its walls (13) triggered by the binding of ATP and, for bacterial and organellar chaperonins, of a cochaperonin (Hsp10) lid (5–7, 13).

Folding in this favorable environment proceeds for a period governed by a timer: the rate of ATP hydrolysis (14). After hydrolysis, ligands, including polypeptide, in either folded or nonnative forms (15, 16), are released from the ring by the binding of ATP to the opposite ring (14), a function of the anticooperativity of ATP binding between rings (17), which places them out of phase with respect to each other in actions of polypeptide binding and folding. Thus, at the chaperonin machine, as for others, the energy of ATP binding is used to effect work, here either of nucleating the folding-active state when binding to the same ring as polypeptide or of dissociating the folding-active state when binding to the opposite ring. ATP hydrolysis, by contrast, is used to directionally advance the machine from its folding-active state toward the binding-active state. Notably, the longest part of the ATP-driven chaperonin reaction cycle ($t_{1/2} \approx 10$ sec) is the folding-active ATP-bound (and cochaperonin-bound) state (18). The hydrolysis timer appears to be slow enough to optimize the ability of proteins to fold in the enclosed cavity, but it also has to be sufficiently fast to release polypeptides from the chaperonin, allowing them, for example, to assemble with partners into oligomeric protein, but more generally to be accessible in the cell to carry out work.

Cavity-Mediated Folding by GroEL

Binding-Active State. The cavity of a ring of bacterial GroEL, the chaperonin studied in greatest depth, transits in any given folding cycle between two major states, a binding-proficient one and a

Freely available online through the PNAS open access option.

Abbreviations: MDH, malate dehydrogenase; DHFR, dihydrofolate reductase; FRET, fluorescence resonance energy transfer.

See accompanying Biography on page 15002.

‡Present address: Chemical Resources Laboratory, Tokyo Institute of Technology, Yokohama 226-8503, Japan.

¶Present address: Laboratory of Molecular Neurobiology and Biophysics, Rockefeller University, New York, NY 10021.

‖To whom correspondence should be addressed. E-mail: horwich@csb.yale.edu.

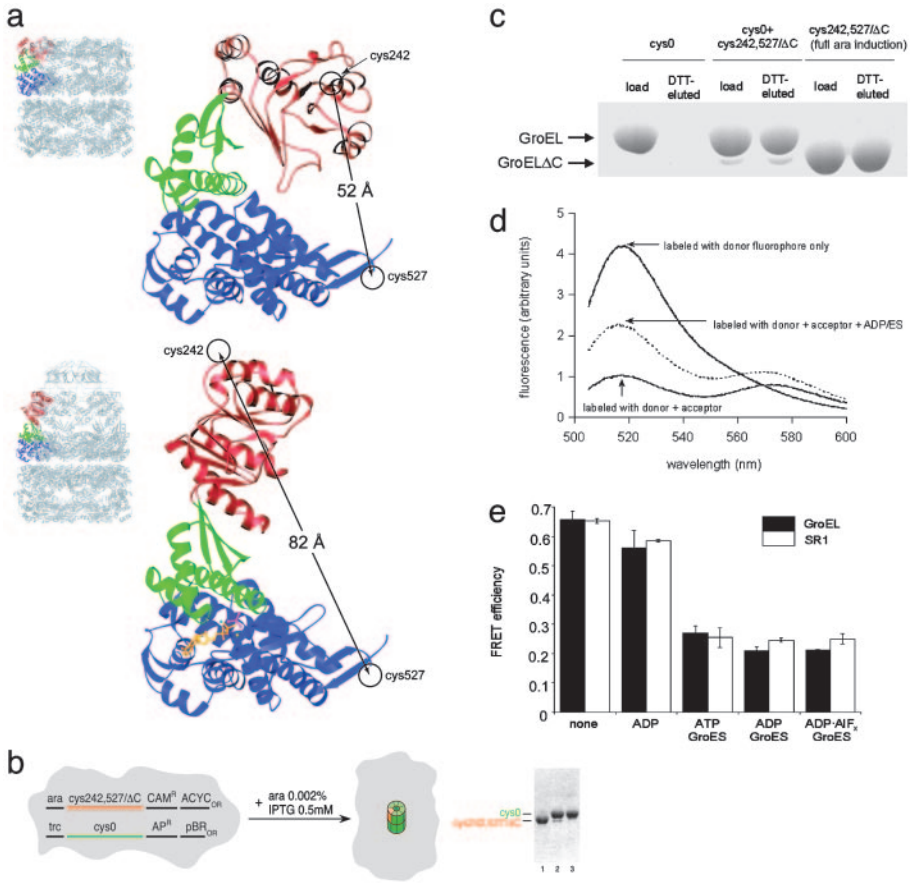

Fig. 1. Construction and analysis of chaperonin complexes containing a fluorescent donor/acceptor-labeled subunit that reports apical domain movement by FRET. (*a*) Positions of two GroEL residues substituted with Cys that were used as sites for attachment of fluorophores, in a subunit of an unliganded ring and in a GroES–ADP–AlF_3-bound subunit. (*Left*) The small ribbon images show intact GroEL (*Upper*) and GroEL–GroES–ADP-AlF_x (*Lower*) complexes, highlighting the individual subunits shown *Right*. The distances shown were measured in the program O (45) between the position of the β-carbon of Lys242, which was replaced here with Cys, and the β-carbon of a Cys residue modeled to extend by an additional residue the terminal strand of GroEL present in electron density in the monoclinic structure (38). The circles drawn connote a diameter of 6 Å around these β-carbon positions. (*b*) Production *in vivo* of complexes bearing a single Cys-substituted subunit, marked by deletion of its COOH terminus, by relative cooverexpression of a full-length Cys0 subunit. (*Left*) The two encoding plasmids and the relative levels of inducers. (*Right*) SDS/PAGE analysis showing overproduction of the truncated Cys-substituted subunit, Cys242,527/ΔC (lane 1), coexpression of the two subunits with relative overexpression of the Cys0 subunit (lane 2), and overexpression of the Cys0 subunit (lane 3). (*c*) Demonstration by SDS/PAGE that the native complexes produced *in vivo* contain the same mixture of subunits observed in *b* when captured through Cys residues under oxidizing conditions on thiopropyl Sepharose, which only retains GroEL with subunits containing Cys. As shown in the middle two lanes, the relative ratio of Cys242,527/ΔC-substituted and Cys0 subunits was identical in the loaded extract (leftmost lane) and after elution from the thiopropyl resin with DTT (rightmost lane). (*d*) Fluorescence emission spectra of mixed subunit GroEL complex labeled with donor fluorophore (fluorescein) only or with both donor and acceptor (tetramethylrhodamine). Donor emission at the maximum of 520 nm was quenched by the presence of acceptor (see time-resolved data in Fig. 4 for decay curves showing that this quench is a function of FRET). The emission of the donor/acceptor-labeled molecules was dequenched by addition of ADP–GroES, indicating a decrease in FRET and an increased distance between the fluorescent labels. (*e*) FRET efficiency estimated from the emission at 520 nm in curves similar to those in *d* and determined in the presence of ADP alone [which produces only small excursions of the GroEL apical domains as observed in a cryoelectron microscopy study (12)] and various combinations of nucleotide and GroES that produce GroES-bound asymmetric complexes whose apical domains are fully elevated and twisted, demonstrating a large change of FRET efficiency associated with nucleotide/GroES binding. Three different labeled preparations of tetradecamer GroEL (filled bars) or single-ring SR1 (open bars) were used for each measurement; the averages are plotted along with the error bars, which show standard deviations.

folding-active state (see Fig. 1*a*) (19). In the binding state, the open polypeptide-accepting form of a GroEL ring exposes a hydrophobic surface at its apical cavity aspect (20, 21), and this surface can multivalently bind nonnative polypeptide through exposed hydrophobic surfaces (22). Such binding to the exposed hydrophobic surfaces of a nonnative protein prevents those surfaces from forming multimolecular interactions with other proteins, which can lead to irreversible aggregation. The multivalent nature of binding, involving contact of the substrate by multiple surrounding apical domains of a GroEL ring (22), may serve to keep the bound protein in a relatively loosely structured state, as indicated by hydrogen exchange and recent NMR experiments (19). In addition, such binding may potentially catalyze unfolding of the substrate protein (23). Unfolding seems likely to result from a so-called thermodynamic partitioning mechanism, in which GroEL preferentially binds less-folded states, thus shifting through mass action the collective of nonnative forms toward relatively less folded ones that bind better (24, 25). Thus, the presence of GroEL can rescue incipiently misfolding states, probably including low-order aggregates that spontaneously dissociate into monomers that can be bound (26). Similarly, GroEL may also bind on-pathway intermediate states that expose significant hydrophobic surface in the context of a collapsed, loosely structured state.

Folding-Active State. In the presence of ATP and cochaperonin GroES, a major transition occurs in a polypeptide-bound GroEL ring (12, 13). Small rigid-body movements of the intermediate and apical domains of the ring attendant to cooperative binding of ATP in the seven equatorial sites cause an initial degree of apical domain elevation and twist (27). These movements are followed by rapid and stable binding of GroES, occurring in well under 1 sec (18), associated with a very large further excursion, such that the apical domains ultimately have undergone an elevation of 60° and clockwise twist of 90° from their unliganded position (13). This excursion effectively moves the hydrophobic polypeptide binding surface entirely away from the central cavity and concomitantly releases polypeptide substrate into it (7, 14). The hydrophobic surface now forms contacts with GroES, in particular with the mobile loops extending from the body of the cochaperonin, which now assume a stable β-hairpin configuration, contacting the hydrophobic apical surface by means of one edge (28, 29). Another portion of the hydrophobic surface becomes involved in a new interface between neighboring apical domains (29). The released polypeptide folds inside this encapsulated chamber in isolation, where it cannot aggregate. Furthermore, the cavity walls of this encapsulated chamber likely favor productive folding. As a result of the rigid-body movements, the surface has switched from its original hydrophobic

character to a hydrophilic character, which may favor burial of hydrophobic surfaces in the folding substrate and exposure of hydrophilic surfaces, properties of the native state. The cavity walls also provide a state of close confinement in a "cage," preventing population of various states (for example, extended ones) that could not be physically accommodated (30). This confinement may effectively "smooth" the energy landscape down which folding proceeds to the native state. To summarize, then, the central cavity of GroEL provides a privileged environment that supports productive folding both through capture of the nonnative states of a large number of different proteins and through support of their productive folding in a favorable environment produced upon encapsulation by the cochaperonin GroES.

A Current Conundrum: ATP/GroES and ADP/GroES End-States Have the Same Structure, but Only ATP/GroES Is Folding-Active

Here we present experiments dealing with the nature of the transition from the binding-active state of GroEL to its folding-productive state. In particular, we present the resolution of a conundrum that has clouded our understanding of the chaperonin system for the past several years. This problem concerns structural observations from both x-ray studies and solution cryoelectron microscopy that the same asymmetric GroEL–GroES end-state is reached when either ATP or ADP nucleotide is supplied (refs. 13 and 29 and N. Ranson, personal communication). This similarity has been confusing, because we and others (e.g., refs. 31 and 32) have observed repeatedly that only ATP will support productive folding of the most stringent GroEL/GroES-dependent substrate proteins, whereas ADP will not. Despite these findings, it was also established in early studies that GroES can bind to GroEL in the presence of ADP (33) and that this can take place even in the presence of substrate protein, allowing, for example, the observation that the encapsulated substrate protein is resistant to digestion by exogenously added protease (5). On the other hand, many experiments show that although substrate is encapsulated inside such ADP GroEL–GroES ternary complexes, it is not released from the cavity wall and, therefore, does not undergo steps of folding. For example, addition of ATP and GroES produces a rapid drop of fluorescence anisotropy of endogenous tryptophans in GroEL-bound ribulose-1,5-bisphosphate carboxylase/oxygenase (14) or of GroEL-bound pyrene-labeled rhodanese (7), commencing within the dead time of mixing (<50 msec). By contrast, addition of ADP and GroES fails to promote any change in anisotropy of either substrate over 10 min. These observations, then, suggest that there should be significant structural differences between ATP and ADP GroEL–GroES complexes; yet none have been observed. By using fluorescence resonance energy transfer (FRET) to monitor in real time the opening movements of the apical domains of GroEL, we show that there is a significant difference in the rates and even the extents of apical domain movement in ATP versus ADP but only in the presence of bound substrate protein. Polypeptide thus appears to comprise a load on the apical domains that can only be overcome by the additional energy supplied by the γ-phosphate of ATP.

Materials and Methods

Proteins. To produce mixed GroEL complexes, Cys0 GroEL (C138A, C458A, and C519A) in the pTrc99m vector (Amp^R and *trc* promoter) and Cys242,527/ΔC GroEL in a pACYC vector (Cam^R with an introduced *ara* promoter) were transformed simultaneously into the Top10 *Escherichia coli* strain. Expression of mixed complexes containing approximately one Cys242,527/ΔC subunit in an otherwise Cys0 GroEL oligomer or Cys0 SR1 oligomer was induced with 0.5 mM isopropyl β-D-thiogalactoside and 0.002% L-arabinose for 3 h at 37°C. The ratio between Cys242,527/ΔC and Cys0 subunits was estimated from the ratio of band intensities of Coomassie-stained SDS/PAGE gels (0.06 for Cys0 + Cys242,527/ΔC, 0.10 for SR1 Cys0 + Cys242,527/ΔC; e.g., Fig. 1*c*). Mixed complexes were purified by Q Sepharose FF and SOURCE 15 ISO chromatography (22) and incubated with Affi-Gel blue (Bio-Rad) in 50 mM Tris, pH 7.5/1 mM DTT containing 20% methanol for 2 h at 25°C to "strip" residual *in vivo*-bound proteins. Purified complexes were dialyzed against 50 mM Tris, pH 7.5/50 mM KCl/1 mM tris(carboxyethyl)phosphine before labeling. GroES Cys98 was produced as described (18). Pig heart mitochondrial malate dehydrogenase and hexokinase were purchased from Roche Applied Science. Bovine rhodanese (7) and human dihydrofolate reductase (DHFR) (34) were expressed and purified as reported.

Binary Complex Formation. Malate dehydrogenase (MDH), rhodanese, and DHFR were denatured in 9 M urea/50 mM Tris, pH 7.5/10 mM DTT for 30 min at 37°C. Binary complexes were formed between mixed GroEL or SR1 oligomers and the substrate proteins by rapidly diluting the denatured protein 100-fold into a solution of 0.2 μM GroEL or SR1 in buffer A (50 mM Tris, pH 7.5/50 mM KCl/10 mM $MgCl_2$/1 mM DTT), such that the final concentrations of substrate protein subunits were 1.0 or 0.5 μM in the mixtures with GroEL or SR1, respectively. After 10 min at 25°C, the mixtures were centrifuged to remove aggregated excess substrate protein. Refolding experiments showed that GroEL and SR1 were essentially saturated with substrate protein under these conditions.

Fluorescence Labeling. GroEL (10 μM) was labeled with 100 μM fluorescein maleimide (Molecular Probes) in 50 mM Tris, pH 7.5/50 mM KCl/0.2 mM tris(carboxyethyl)phosphine/20% glycerol for 24 h at 4°C. The reaction was quenched by addition of 1 mM DTT. Unreacted labeling reagent was removed by ultrafiltration and gel filtration on a PD-10 column (Amersham Pharmacia) equilibrated with the same buffer. The GroEL fraction was reacted with 10 μM tetramethylrhodamine maleimide (Molecular Probes) at 4° for 48 h and purified by the same procedure. The labeling efficiency was estimated from absorbance at 491 nm for fluorescein (ε = 83,000 $M^{-1}\cdot cm^{-1}$) and 541 for tetramethylrhodamine (ε = 95,000 $M^{-1}\cdot cm^{-1}$). The fraction of molecules labeled only with donor and with both fluorescent labels was calculated from the fluorescence lifetime measurements (Fig. 4, which is published as supporting information on the PNAS web site).

Fluorescence Lifetime Measurements. Fluorescence lifetimes were measured by using a time-domain fluorometer (Photon Technology International, Lawrenceville, NJ). Excitation from the dye laser was at 490 nm, filtered through a short-wave pass filter (catalog no. R00910-00, Reynard, San Clemente, CA). Samples were measured under the same conditions as in the steady-state fluorescence experiments below; for samples with GroES and ATP, fluorescence lifetimes were measured after the steady-state fluorescence change had reached equilibrium. Amplitude, fractional intensity, and lifetime parameters were calculated by a nonlinear least-squares procedure (35) with software from the Center for Fluorescence Spectroscopy (cfs.umbi.umd.edu/cfs/). Distances were estimated by using the Förster equation, $r = R_0[(1/(1 - \tau_{DA}/\tau_D) - 1)]^{1/6}$, where the Förster distance, R_0, was assumed to be 54 Å (36).

Steady-State and Stopped-Flow FRET. Steady-state fluorescence measurements were taken on a QM-1 fluorescence spectrometer (Photon Technology International). Solutions contained 0.02 μM chaperonin or 0.02 μM chaperonin–polypeptide binary complexes in buffer A; 0.1 μM GroES and 1 mM nucleotide were added and mixed manually. When ADP was used, 0.01 units/μl hexokinase and 100 mM glucose were added to hydrolyze any contaminating ATP (37). Where indicated, 0.2 mM $KAl(SO_4)_2$ and 5 mM KF were also added. Note that these concentrations are about 1/10th those used to form AlF_x for functional studies in ref. 13, necessitated to prevent precipitation in the cuvette. A slower rate of refolding is associated with this concentration. Excitation of the donor was at

490 nm, and emission was measured at 520 nm, where no appreciable acceptor fluorescence emission occurs.

The stopped-flow apparatus has been described in ref. 14. Assays were carried out under the same buffer conditions as for the steady-state FRET measurements. The excitation wavelength was 475 nm. Emission light was filtered by a green color separation filter (catalog no. R01945-00, Reynard), a short-wave pass filter (catalog no. R00915-00, Reynard), and a long-pass barrier filter (catalog no. GG495, Schott, Duryea, PA). Data were analyzed by a least-squares fitting procedure (Kaleidagraph, Reading, PA).

Results

Placement of Fluorophores That Report Apical Domain Movement by FRET. ***Strategy and production of labeled GroEL molecules.*** To monitor GroEL apical domain movements in real time, we placed a donor–acceptor pair of fluorophores at two distinct positions within the same GroEL subunit, selected such that their separation in an unliganded GroEL ring would produce FRET that would change substantially upon transition to a GroES-bound state (Fig. 1*a*). The two positions for labeling were selected by examination of the crystal structures of unliganded GroEL (20) and GroEL-GroES-ADP-AlF_3, the latter recently shown to structurally and functionally mimic an ATP/GroES-bound state (13). Asn527 lies at the inside aspect of the stable equatorial "base" of the GroEL subunit, comprising the first residue of the flexible COOH-terminal tail of the GroEL subunit (Fig. 1*a*). Although not crystallographically resolvable (the last resolvable residue is Lys526) (38), it would, nevertheless, be predicted to lie near the wall of the cavity, i.e., within ≈4 Å of residue 526, which lies just inside the wall. Because the resolvable portion of the equatorial domain does not undergo any significant structural change upon nucleotide/GroES binding to GroEL (Fig. 1*a*), we predicted that residue 527 would itself be relatively fixed in position. By contrast, the other residue chosen, Lys242, which lies at the top of the cavity-facing aspect of the apical domain of unliganded GroEL at the COOH-terminal end of an α-helix involved in polypeptide binding (helix H), undergoes a major movement through space upon nucleotide/GroES binding. Lys242 is elevated and rotated away from its original position, as part of the rigid-body movement of the apical domain, to a position where its side chain points out from the top of the GroEL portion of the GroES-bound (cis) ring into the bulk solution, increasing its distance from residue 527 from ≈52 Å to ≈82 Å (Fig. 1*a*).

Residues 242 and 527 were altered to Cys in a Cys0 version of GroEL (Cys0) (14) and, in addition, the COOH-terminal residues beyond residue 527 (amino acids 528–547) were deleted to enable ready identification of the substituted subunit. The altered subunit, Cys242,527/ΔC, was shown to be fully functional, insofar as its expression could rescue growth of a GroEL-deficient strain (data not shown). To simplify interpretation of FRET data, we wished to limit potential modification sites to only one subunit in any given GroEL tetradecamer. This arrangement was accomplished by coexpressing Cys242,527/ΔC at a relatively low level from an *ara* promoter and Cys0 full-length GroEL (wild type at residues 242 and 527) at a high level from a *trc* promoter in the same cell strain (Fig. 1*b*). SDS/PAGE analysis of cells that had been directly solubilized revealed an ≈15-fold excess of the Cys0 full-length subunit over the Cys242,527/ΔC subunit (Fig. 1*b*).

To demonstrate that the complexes were indeed mixed in character, the Cys-containing complexes were captured under oxidizing conditions on a thiopropyl Sepharose resin and were then recovered by reduction. The same relative ratio of full-length to deleted subunits was observed in the recovered complexes as in the loaded material (Fig. 1*c*, middle two lanes, compare load and DTT-eluted), indicating that the full-length, Cys0 subunits were coassembled in the observed ratio with the deleted, Cys-substituted ones.

The complexes were labeled with donor and acceptor fluorophores fluorescein and tetramethylrhodamine, respectively, in sequence: first the donor and then the acceptor (see *Materials and Methods*). This protocol was expected to produce a mixed population of fluorescently labeled molecules, a portion of which would be heterologously labeled with donor at one position and acceptor at the other and another portion of which would have the donor (or the acceptor) fluorophore at both positions. Fluorescence lifetime studies (Fig. 4*a*), which examined decay of donor fluorescence of the products of the double-labeling reaction, indeed revealed two different single exponential rates of decay: one with a slower rate (τ_1 = 4.09 nsec) also observed for the sample labeled only with donor, which accounted for 36% of the reporting molecules in the double-labeled sample and a second, more rapid rate (τ_2 = 1.35 nsec) observed only for the double-labeled sample, which reflected FRET between the donor and acceptor fluorophores and involved 64% of the donor-labeled molecules. Note that molecules labeled only with acceptor do not contribute to this and the following analyses. The FRET efficiency calculated from these time constants is 0.67, which can be used to estimate an interfluor distance of ≈50 Å (see *Materials and Methods*). This finding is consistent with the distance between residues 242 and 527 in unliganded GroEL estimated from the crystallographic model (≈52 Å).

Observation of FRET and change of efficiency caused by binding GroES. The steady-state fluorescence emission spectra, excited at the donor excitation maximum, of complexes labeled only with the donor fluorophore or labeled with both fluorophores were determined (Fig. 1*d*). Consistent with occurrence of FRET in the double-labeled complexes, as apparent from the fluorescence decay studies, the fluorescence intensity of the double-labeled molecules at the donor emission maximum (520 nm) was substantially quenched relative to that of the single-labeled ones. Whereas addition of ADP and GroES did not affect the molecules labeled only with the donor fluorophore (data not shown), when added to the double-labeled molecules, there was an increase of fluorescence at the donor emission maximum (Fig. 1*d*), reflecting dequenching of the donor and decreased FRET efficiency, as predicted from the increase of distance between donor and acceptor as a result of the conformational change in GroEL. FRET efficiency could be quantitated from similar experiments using various nucleotides and GroES (Fig. 1*e*, solid bars), correcting for the contribution of the molecules in the double-labeled population that were only labeled with the donor fluorophore (see *Materials and Methods*). From these calculations, ATP/GroES binding produced a reduction in FRET efficiency from ≈65% to ≈27% (Fig. 1*e*). Notably, when ATP/GroES is added to GroEL, it produces a cycling reaction in which 50% of the rings bearing a fluorescent subunit are unoccupied by GroES at any given time (assuming one labeled subunit per GroEL molecule) and adopt the unliganded conformation. Thus, the FRET change must come from the ≈50% of molecules that are GroES-bound at any given time. Consistent with this finding, the fluorescence decay curve of such a sample (Fig. 4*a*, panel 4) could be best fit by the sum of three exponentials: as before, one for a ring with a donor-only-labeled subunit (τ_1 = 4.09 nsec) and one for a ring with a double-labeled subunit in the unliganded state (τ_2 = 1.35 nsec) but also an additional one for a double-labeled subunit in a GroES-liganded ring (τ_3 = 2.94 nsec), each accounting for about one-third of the labeled population. Furthermore, when ADP/GroES or ADP-AlF_x/GroES was added, producing stable asymmetric GroEL-GroES complexes in which GroES becomes randomly associated with one ring of GroEL, either the same ring as the fluorescent subunit or the opposite one, the same reduction of FRET efficiency relative to GroEL alone was obtained (Fig. 1*e*) and the same decay curves were seen (see Fig. 4*a* for ADP/GroES).

As further evidence that the FRET change reflects principally, if not exclusively, the formation of GroES-bound GroEL rings, SR1, a single-ring version of GroEL that binds GroES stably in the presence of ATP, was similarly modified, labeled, and studied. When ATP and GroES were incubated with labeled SR1 as in the preceding experiments, a nearly identical change in FRET efficiency was observed (Fig. 1*e*, open bars). Here, however, the

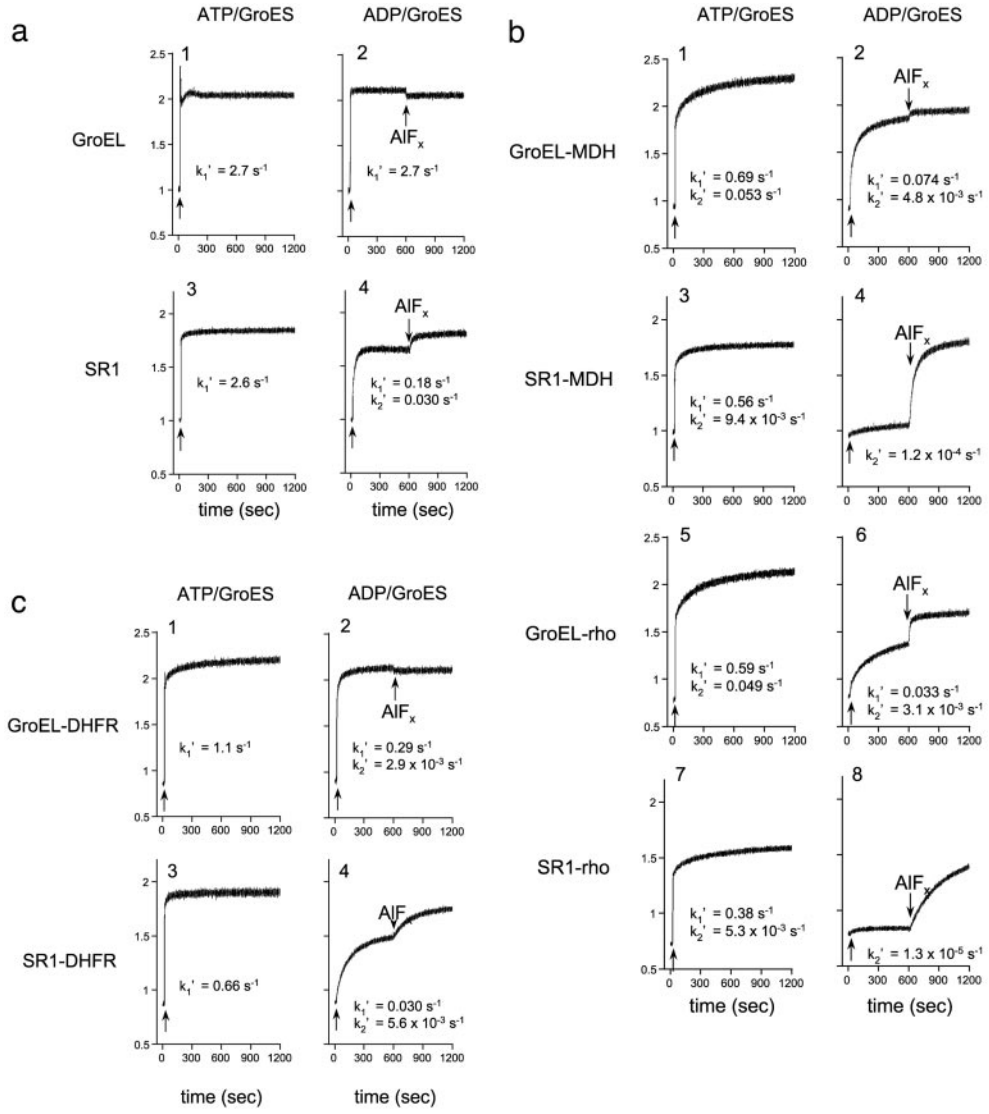

Fig. 2. Time course of change in FRET in the presence of nucleotides, GroES, and bound substrate polypeptides. (*a*) Addition of GroES and either ATP (panels 1 and 3) or ADP (panels 2 and 4) to both GroEL (panels 1 and 2) and SR1 (panels 3 and 4), without bound polypeptide, results in a rapid change in FRET. GroES (0.1 μM) and nucleotide (1 mM) were added to 0.02 μM chaperonin with manual mixing; $KAl(SO_4)_2$ and KF were added to final concentrations of 0.2 mM and 5 mM, respectively, to form AlF_x where indicated. (*b*) Addition of GroES and either ATP (panels 1, 3, 5, and 7) or ADP (panels 2, 4, 6, and 8) to binary complexes of GroEL and SR1 with substrate polypeptides results in reduced rates and extents of FRET change, particularly with ADP. GroES and nucleotide were added as in *a* to 0.02 μM binary complexes of GroEL or SR1 and MDH (panels 1–4) or rhodanese (rho) (panels 5–8) with manual mixing; AlF_x was formed as above and added where indicated. (*c*) Addition of GroES and either nucleotide to binary complexes of chaperonins with DHFR, a less tightly bound substrate polypeptide, results in greater rates of FRET change. Experiments were carried out as in *b*, except with 0.02 μM chaperonin–DHFR binary complexes. For all experiments, excitation was at 490 nm and emission was at 520 nm. The scale of the ordinate is in arbitrary fluorescence units. In each case, a representative set of traces is presented. The major apparent rate constants are included on each trace; for clarity, those accounting for <15% of the observed amplitude are not presented.

fluorescence decay curve was fit by only two exponentials (Fig. 4*b*), reflecting the expected presence of only two populations of molecules: those labeled only with donor ($\tau = 4.09$ nsec) and those with a double-labeled subunit in a GroES-liganded ring ($\tau = 2.95$ nsec). Note that the presence of GroES does not affect the fluorescence decay of the population of molecules that had received only the donor fluorophore in the double-labeled sample.

Time-Dependent Changes of FRET: Presence of Substrate Polypeptide Drastically Slows Apical Movement in ADP/GroES. ***FRET changes in the absence of substrate.*** The changes in steady-state FRET upon nucleotide/GroES binding to both GroEL and SR1 were also monitored in a time-dependent manner (Fig. 2). We observed that ATP/GroES produced the FRET change rapidly, within a second of addition (Fig. 2*a*, panels 1 and 3). The changes were more accurately observed with stopped-flow mixing (Table 1 and Fig. 5, which is published as supporting information on the PNAS web site). The kinetics of the FRET change with GroEL involved a rapid increase ($k_1 = 2.7\ s^{-1}$) leading to an overshoot of the final amplitude followed by a decrease and slight rebound. For SR1, there was a similarly rapid rise ($k_1 = 2.6\ s^{-1}$) but no overshoot, leading us to conclude that the overshoot observed with GroEL is likely the result of transient binding of ATP or ATP/GroES to the

Table 1. Apparent kinetic constants of FRET change

	Nucleotide/GroES binding to GroEL				Nucleotide/GroES binding to SR1			
	ATP		ADP		ATP		ADP	
	k_1'	k_2'	k_1'	k_2'	k_1'	k_2'	k_1'	k_2'
No substrate	2.7 (100)	—	2.7 (100)	—	2.6 (93)	1.0×10^{-3} (7)	0.18 (32)	3.0×10^{-2} (68)
MDH	0.69 (72)	5.3×10^{-2} (28)	7.4×10^{-2} (34)	4.8×10^{-3} (66)	0.56 (79)	9.4×10^{-3} (21)	1.0×10^{-2} (4)	1.2×10^{-4} (96)
Rhodanese	0.59 (68)	4.9×10^{-2} (32)	3.3×10^{-2} (26)	3.1×10^{-3} (74)	0.38 (79)	5.3×10^{-3} (21)	1.6×10^{-2} (5)	1.3×10^{-5} (95)
DHFR	1.1 (86)	6.7×10^{-3} (14)	0.29 (79)	2.9×10^{-3} (21)	0.66 (91)	1.9×10^{-3} (9)	3.0×10^{-2} (24)	5.6×10^{-3} (76)

The percentage of total intensity change accounted for by each rate constant is shown in parentheses. —, Not observed.

open trans ring (see Fig. 5 legend). When ADP/GroES was added to GroEL, a change of the same magnitude on the same time scale as with ATP/GroES addition was observed, with $k_1 = 2.7\ s^{-1}$ (Fig. 2*a*, panel 2) and no overshoot. With SR1, the change produced by ADP/GroES addition was slower overall but of the same magnitude, and two rates of similar amplitude were apparent: $k_1' = 0.18\ s^{-1}$ and $k_2' = 0.03\ s^{-1}$ (Fig. 2*a*, panel 4, and Table 1). Adding AlF_x to mimic the γ-phosphate of ATP to either of these ADP complexes after the maximum fluorescence was reached led to only a minimal additional change in FRET (Fig. 2*a*, panels 2 and 4).

These data suggest that either ATP or ADP (or ADP/AlF_x) in the presence of GroES can support rapid and full excursion of the apical domains of GroEL to form an asymmetric GroEL–GroES complex. Furthermore, both nucleotides similarly support these changes in SR1, although ADP produces a somewhat slower rate, albeit with the same ultimate extent of change. Consistent with these observations, particularly as they relate to the extent of change, the structures of the apical and intermediate domains, as well as those of GroES, in these end-states are identical, as determined crystallographically in GroEL-GroES-ADP-AlF_3 (13), GroEL-GroES-ADP (29), and SR1-GroES-ADP-AlF_3 (13) complexes and by cryoelectron microscopy for hydrolysis-defective GroEL D398A-GroES-ATP and GroEL-GroES-ADP (N. Ranson, personal communication).

FRET changes in the presence of substrate protein. The behavior of the change in FRET was quite different upon nucleotide/GroES addition to GroEL or SR1 complexes occupied with bound polypeptide substrate (Fig. 2*b*). For both GroEL and SR1, occupancy with either MDH or rhodanese slowed the rate of FRET change, suggesting an effect of polypeptide on the rate of apical domain excursion. When ATP/GroES was added (Fig. 2*b*, panels 1, 3, 5, and 7), the rate was reduced 4- to 6-fold (Table 1), although the magnitudes of the changes were similar to those in the absence of polypeptide. Here again, slight overshoots could be observed with GroEL and not SR1 (Fig. 5), and second rate constants with relatively small amplitudes were required to fit the longer-term data (Table 1). These results are consistent with earlier studies showing release of polypeptide from the apical binding sites on the same time scale (<1 sec) upon ATP/GroES addition to polypeptide–GroEL binary complexes (7, 13, 14).

In striking contrast, when ADP/GroES was added to substrate-bound GroEL binary complexes (Fig. 2*b*, panels 2, 4, 6, and 8), the overall changes of FRET were much slower and had two phases: a minor phase ($t_{1/2} \approx 10$–20 sec) and a prominent, very slow phase ($t_{1/2} \approx 150$–250 sec), accounting for 65–75% of the change (Fig. 2*b*, panels 2 and 6, and Table 1). In the case of MDH, the half-maximum amplitude was reached only after 50 sec, instead of 1–2 sec in GroES/ATP (Fig. 2*b*, compare panel 2 with panel 1). In the case of rhodanese, even after 10 min, the donor fluorescence failed to reach the point achieved by ATP/GroES addition within 10 sec (Fig. 2, compare panel 6 with panel 5). For SR1–substrate binary complexes, the situation was even more extreme, with only slowly occurring, small amplitude changes in FRET (Fig. 2*b*, panels 4 and 8). The apical movements reflected in the observed FRET change appear to be both retarded in rate and limited in extent of excursion. Nevertheless, it appears that the molecules remain able to make the full excursion if subsequently supplied with AlF_3 complex, mimicking the γ-phosphate of ATP. For example, as shown in Fig. 2*b*, panel 6, when AlF_x was added 600 sec after ADP/GroES addition to GroEL–rhodanese complexes, there was a rapid (<10 sec) FRET change to the full extent observed when AlF_x was added initially with ADP/GroES (data not shown). With SR1 complexes, AlF_x addition after ADP/GroES produced slower rates of FRET change than seen with ATP, but they were still fast enough to be consistent with the observed rates of protein folding at SR1 under these conditions, which used a relatively low concentration of AlF_x (see *Materials and Methods*).

In summary, when incubated with polypeptide-bound GroEL or SR1 complexes, ADP/GroES failed to produce an efficient excursion of the apical domains to their fully open, GroES-bound position. This finding is consistent with the recognized inability of ADP/GroES to trigger productive folding of these substrate proteins, associated with a failure of polypeptide to be released from the cavity wall, determined by earlier fluorescence anisotropy and gel filtration experiments (7, 13, 14). Such release fails to occur despite the apparent ability of GroES to bind to such binary complexes as evidenced, for example, by acquired protection of rhodanese or MDH from exogenous protease (5, 39).

A nonstringent substrate, DHFR, does not impose a load. As a correlate to the conclusion that multivalently bound substrates like MDH and rhodanese impose a substantial load on the GroEL apical domains, we would predict that a less tightly bound substrate, such as DHFR, might impose a lighter load. We previously observed in studies of GroEL rings bearing various numbers of binding-defective apical domains that DHFR requires only two binding-competent apical domains for efficient GroEL-dependent binding (G.W.F., unpublished data). Consistent with this, when ADP/GroES was added to a GroEL–DHFR binary complex, the predominant rate of the FRET change observed was much faster (60- to 100-fold) than those of the major (slower) phases for MDH and rhodanese (Fig. 2, compare *c*, panel 2, with *b*, panels 2 and 6). This observation reflects the ability of ADP/GroES to trigger release and productive cis folding of DHFR (6, 32), whereas it fails to do so for MDH or rhodanese (7, 14). Similarly, when the same experiment was carried out with SR1, the FRET change occurred far more rapidly than with MDH or rhodanese (Fig. 2, compare *c*, panel 4, with *b*, panels 4 and 8), albeit more slowly than at GroEL.

GroES associates with GroEL-substrate at a faster rate than apical domain movement occurs. What is the potential role of the arrival of GroES itself in bringing about these apical movements? Does GroES, for example, begin to interact with GroEL before apical domain movement is complete, or, conversely, must apical domain movement be completed before GroES can associate, with the rate of opening before GroES binding determining the outcomes observed for the different nucleotides? FRET experiments were carried out that examined binding between donor-labeled SR1 (Cys242,527), obligately cis-forming, and varying concentrations of acceptor-labeled GroES Cys98 in the presence of ATP. We observed that the apparent rate of GroES binding to SR1 was rapid ($2.6 \times 10^7\ M^{-1}{\cdot}s^{-1}$), whereas the presence of MDH or rhodanese caused a 2- to 3-fold slowing in the rate of association (Fig. 3*a*). By contrast, the rate of apical domain opening was more strongly affected by the presence of substrate, consistent with the idea that substrate comprises a load on the system. In the absence of substrate, the rate of apical opening was virtually the same as the rate of GroES arrival ($2.8 \times 10^7\ M^{-1}{\cdot}s^{-1}$) (Fig. 3, compare *c* with *a*), but in the presence of substrate, the rate of apical domain opening was slowed by 4-to 20-fold relative to that in the absence of substrate, depending on the particular substrate protein and on the concentration of GroES. Thus, in the presence of substrate, GroES arrival occurs before the apical domains are fully opened, implying the initial formation of a collision complex with GroEL, in which a physical association occurs before apical domain movement is appreciable. In addition, it appears that, given the concentration-dependent ability of GroES to accelerate the rate of apical movement of substrate-bound GroEL (Fig. 3*b*), GroES may play a role in assisting completion of apical domain movement. Nevertheless, in the presence of polypeptide load, the rate of apical domain movement showed saturation behavior relative to GroES concentration, whereas, in the absence of load, it did not. Thus, GroES binding can only provide opposition to the polypeptide load to a certain extent.

Discussion

Role of the γ-Phosphate of ATP in Opposing a Load from Bound Substrate Polypeptide. The above findings suggest that polypeptide binding by a GroEL ring imposes a load on the apical domains that

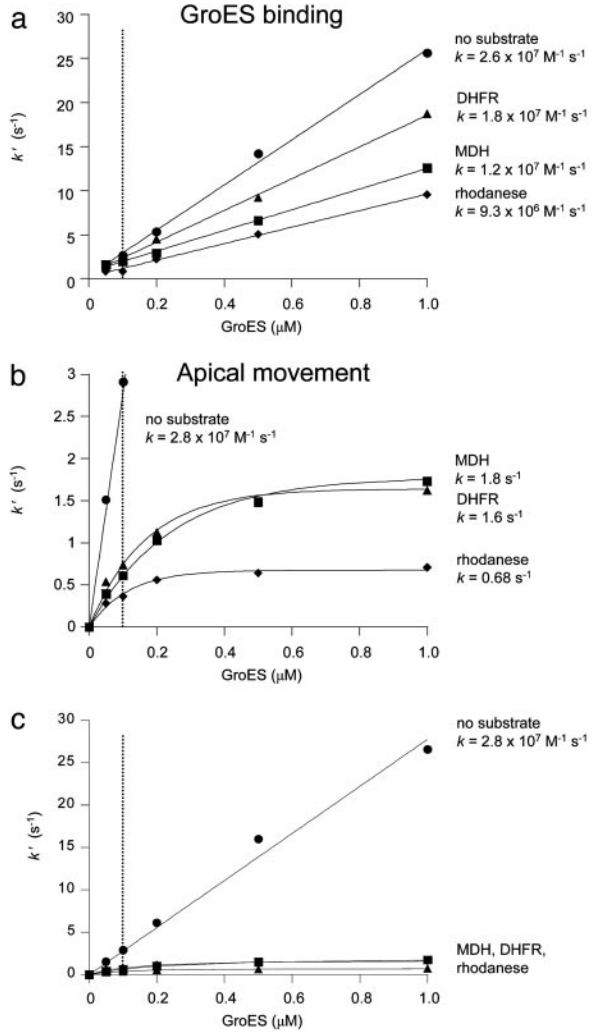

Fig. 3. Rates of GroES binding (*a*) and apical domain movement of SR1 as a function of GroES concentration (*b* and *c*). (*a*) Stopped-flow experiments were carried out as stated for Fig. 5, except with fluorescein-labeled Cys242,527 SR1 and tetramethylrhodamine-labeled GroES Cys98 in the presence of ATP, observing the acquisition of FRET (decrease in donor emission intensity) as a function of time as GroES became bound to SR1. Both unliganded and polypeptide-bound SR1 showed a linear increase in the observed rate of GroES binding with increasing GroES concentration, consistent with a bimolecular interaction between GroES and SR1. The presence of polypeptide influences this rate moderately (up to 3-fold). (*b*) Stopped-flow experiments monitoring apical domain movement similar to those shown in Fig. 5 were carried out in various concentrations of GroES. In the absence of substrate, the observed rate increases linearly with GroES concentration. In contrast, when polypeptide is bound to the apical domains, the observed rates show saturation behavior, indicating that the rate-determining step in apical movement changes when polypeptide is bound and becomes a process independent of GroES. The data with bound polypeptide were fit to a standard saturation equation by using the major apparent rate constants calculated from the stopped-flow data. (*c*) The same experiments as shown in *b* but with the ordinate expanded 10-fold to show the linearity of the dependence of the observed rate constant with GroES concentration in the absence of substrate. The rate constants shown were calculated from the fits to the data, indicated by the drawn curves. In each panel, the vertical dotted line indicates the concentration of GroES (0.1 μM) at which the experiments in Fig. 2 and Table 1 were performed.

counters the action of nucleotide and GroES in driving apical elevation (60°) and twist (90° clockwise). That is, polypeptide, bound by multiple apical domains (22), may exert a downward and/or inward force on the apical domains. ATP/GroES is able to rapidly and efficiently produce apical movement even in the presence of the polypeptide load, as judged by the observation that 90% of the FRET change occurs within 2–3 sec. Likewise, AlF_3 can accomplish the same action when added to GroEL-GroES-ADP-polypeptide complexes (see Fig. 2*b*). Nevertheless, the rate of movement, even in ATP/GroES, was slowed by ≈4- to 6-fold, as shown by the stopped-flow measurements. But the effect of a load from bound MDH or rhodanese on ADP/GroES movement is profound, with the overall rate vastly slowed (by 150-fold) relative to ATP/GroES. The majority of the amplitude of change was associated with a very slow rate ($t_{1/2} > 150$ sec), far longer than the duration of the entire reaction cycle ($t_{1/2} \approx 10$–15 sec) (18, 40). In addition, the overall extent of movement supported by ADP/GroES in the face of these loads appears to be reduced or minimal, particularly in the case of SR1, as reflected in the magnitude of the FRET changes. For SR1, this more severe effect may be a function of distortion of the SR1 structure, which lacks a stabilizing equatorial interface, under these conditions.

The increment of free energy available for apical movement provided by the binding of the γ-phosphate has been estimated by thermodynamic studies of formation of SR1-GroES-ADP-AlF_3 complexes at ≈43 kcal per mol (1 cal = 4.184 J) of rings (13). This large free-energy change derives from the formation of seven new hydrogen bonds between each of the seven AlF_3 moieties and the corresponding equatorial nucleotide pocket of a ring, as observed from the crystal structure of GroEL-GroES-ADP-AlF_3 (13). This amounts to ≈1 kcal/mol per hydrogen bond, an estimate that agrees with other studies (e.g., ref. 41). This energy is presumably at least partly released as kinetic energy that drives forceful elevation and twisting movement of the apical domains, a "power stroke" responsible for release of substrate polypeptide.

By contrast, the energy of ADP/GroES binding is insufficient to drive apical movements that can eject such substrates as MDH or rhodanese off of the cavity wall. The observations in ADP/GroES of FRET changes that occur on a very long time scale (equal to multiple entire chaperonin cycles) and that are partial in extent suggests that the apical domains do eventually open to some extent, but either their slow rate of movement or the lack of completion of the excursion of movement results in failure to eject bound polypeptide into the cis cavity and in a failure to produce the native state. Failure of substrate ejection has been directly verified experimentally by two different types of experiment. In one experiment, mentioned earlier, the fluorescence anisotropy of bound substrate (rhodanese or ribulose-1,5-bisphosphate carboxylase/oxygenase) failed to undergo any drop upon addition of ADP/GroES as compared with a rapid drop upon addition of ATP/GroES (7, 14). Thus, there is no observable conformational change in the substrate protein promoted by ADP/GroES addition, despite binding and encapsulation by GroES. In a second experiment, ADP–SR1–GroES rhodanese complexes were briefly subjected to cold exposure to release GroES and then gel filtered (13). Rhodanese remained associated with SR1, indicating that the substrate was never released from the cavity wall upon GroES binding in ADP. This result seems to suggest that whereas GroES can associate with GroEL in cis ADP complexes and is able to encapsulate rhodanese, the apical domains may not occupy a structural state in which the apical hydrophobic binding sites are fully displaced from the central cavity. As discussed below, it seems that such cis ADP–GroES–GroEL–polypeptide complexes are trapped either in an initial collision state, where GroES has associated with GroEL but the apical domains have not fully opened, or in a complex that lies in some intermediate state along the pathway to the fully open one.

Evidence for a Collision State of GroES with GroEL: Role in Committing Polypeptide to the GroEL Cavity for a Round of cis Folding. The comparison of the rate of GroES association with GroEL–substrate in ATP versus the rate of apical domain movement, as shown in Fig. 3, makes clear that, in the presence of bound substrate protein, GroES arrives at GroEL before apical domain movement is com-

pleted. The rate of apical movement is slowed by anywhere from 4- to 10-fold relative to the rate of GroES binding, depending on the particular GroEL-bound substrate protein and on the concentration of GroES. The implication is that, in the presence of physiologic nucleotide, ATP, and substrate protein, there is a collision state formed by incoming GroES and the GroEL–substrate complex that precedes the completion of opening of the apical domains. Moreover, because ATP alone does not appear to be able to trigger full apical opening as judged from electron microscopy studies, it appears that GroES is required to enable such an extent of movement to take place. Thus, as implied in the foregoing discussion, the complexes formed by ADP/GroES addition to substrate–GroEL may be stalled in such collision states or intermediate states beyond them that lie along the pathway to full apical opening, states in which polypeptide can be encapsulated underneath GroES but still remains lodged on the apical hydrophobic binding sites.

The nature of these collision or postcollision intermediate states can only be speculated on at present, but one possibility is that in forming the initial collisional association, the mobile loops of GroES directly bind at apical hydrophobic sites that are unoccupied by substrate polypeptide, docking the cochaperonin over the polypeptide-bound ring and ensuring that substrate protein cannot escape once it is released from the cavity wall. Indeed, an earlier study showed that GroES could be bound to a GroEL ring containing only a single intact hydrophobic apical domain, so an initial univalent contact of this sort may be possible (22). Consistent with this as a potential docking site, GroES fails to make any appreciable stable contact with GroEL when all of the apical sites have had their hydrophobic character disrupted (21). An alternative consideration, however, is that initial docking of GroES with GroEL could occur at some other site on the top of the apical domains, but a host of mutational alterations involving this surface have failed to produce any defect of GroES binding (21).

There is additional potential evidence from mutant studies for collision states in which GroES forms an initial association with GroEL–substrate that encapsulates substrate protein but fails to trigger its release and folding. Kawata and coworkers (42) have reported a GroEL mutant, C138W, that is unable to trigger folding of substrates encapsulated with GroES in ATP at 25° but that, upon a shift to 37°C, resumes productive cis folding. It seems likely that at 25°C this ternary GroEL–GroES–substrate complex is trapped in a collision or postcollision intermediate state, as opposed to an off-pathway state. Our own studies have also recently uncovered a further such trapped mutant mapping to the equatorial nucleotide pocket (E. Chapman, G.W.F., and A.L.H., unpublished results). Structural studies of both the ADP–GroEL–GroES–substrate complexes and the stalled substrate–encapsulated mutant complexes should now be informative concerning the collision and postcollisional states. It seems clear, however, from the collective of studies that the initial collision of GroES with GroEL–substrate occurs in such a manner that polypeptide is committed to remain in the cavity of the GroEL ring during the process of apical movement that will eject it off the hydrophobic binding sites. Thus, this collision mechanism prevents substrate protein from release into the bulk solution, where it would misfold and aggregate (30), and assures a trial at productive folding inside the GroES-encapsulated cis cavity.

Nature of the Polypeptide Load on the GroEL Apical Domains. Finally, the nature of the polypeptide load that is overcome by ATP/GroES-driven apical movement needs to be considered. Because little or no stable structure has been observed to date in GroEL-bound substrates as examined by using hydrogen exchange and NMR (19), it seems likely that the load does not lie at the level of polypeptide structure that has to be pulled against but, rather, lies at the level of hydrophobic contacts formed directly between side chains in the nonnative substrate and hydrophobic side chains of the apical domains of GroEL (see, e.g., refs. 43 and 44). Such side chain contacts, which may really be more of a surface-to-surface type of contact and which may occur between substrate and more than one surrounding apical domain simultaneously (22), may collectively account for the need for kinetic force to release substrate polypeptide. In this vein, one can consider, for example, that the affinity of GroEL for a number of substrates, such as MDH and rhodanese, has been estimated to be in the nanomolar range, presumably the convolution of the affinities of individual apical domains for portions of the bound nonnative substrate protein. Significant kinetic force may thus be required to break all of these contacts needed for ejection of the polypeptide substrate as an unbound chain into the cis cavity. By contrast, such substrates as DHFR, making contact with only one or two apical domains of a ring, would not be expected to require as much energetic force to be ejected, in agreement with the observations here that apical movement can proceed with this substrate in the presence of ADP/GroES (Fig. 2*c*). Further structural studies of bound substrate proteins should better resolve the nature of binding and, hence, the nature of bound polypeptide as a load on the system.

1. Anfinsen, C. B. (1973) *Science* **181,** 223–230.
2. Bukau, B. & Horwich, A. L. (1998) *Cell* **92,** 351–366.
3. Hartl, F. U. & Hayer-Hartl, M. (2002) *Science* **295,** 1852–1858.
4. Horwich, A. L., ed. (2002) *Advances in Protein Chemistry*, (Academic, San Diego), Vol. 59.
5. Weissman, J. S., Hohl, C. M., Kovalenko, O., Kashi, Y., Chen, S., Braig, K., Saibil, H. R., Fenton, W. A. & Horwich, A. L. (1995) *Cell* **83,** 577–587.
6. Mayhew, M., da Silva, A. C., Martin, J., Erdjument-Bromage, H., Tempst, P. & Hartl, F. U. (1996) *Nature* **379,** 420–426.
7. Weissman, J. S., Rye, H. S., Fenton, W. A., Beechem, J. M. & Horwich, A. L. (1996) *Cell* **84,** 481–490.
8. Meyer, A. S., Gillespie, J. R., Walther, D., Millet, I. S., Doniach, S. & Frydman, J. (2003) *Cell* **113,** 369–381.
9. Langer, T., Pfeifer, G., Martin, J., Baumeister, W., and Hartl, F. U. (1992) *EMBO J.* **11,** 4757–4765.
10. Braig, K., Simon, M., Furuya, F., Hainfeld, J. F. & Horwich, A. L. (1993) *Proc. Natl. Acad. Sci. USA* **90,** 3978–3982.
11. Thiyagarajan, P., Henderson, S. J. & Joachimiak, A. (1996) *Structure (London)* **4,** 79–88.
12. Roseman, A. M., Chen, S., White, H., Braig, K. & Saibil, H. R. (1996) *Cell* **87,** 241–251.
13. Chaudhry, C., Farr, G. W., Todd, M. J., Rye, H. S., Brunger, A. T., Adams, P. D. & Horwich, A. L. & Sigler, P. B. (2003) *EMBO J.* **22**, 4877–4887.
14. Rye, H. S., Burston, S. G., Fenton, W. A., Beechem, J. M., Xu, Z., Sigler, P. B. & Horwich, A. L. (1997) *Nature* **388,** 792–798.
15. Todd, M. J., Viitanen, P. V. & Lorimer, G. H. (1994) *Science* **265,** 659–666.
16. Weissman, J. S., Kashi, Y., Fenton, W. A. & Horwich, A. L. (1994) *Cell* **78,** 693–702.
17. Yifrach, O. & Horovitz, A. (1995) *Biochemistry* **34,** 5303–5308.
18. Rye, H. S., Roseman, A. M., Chen, S., Furtak, K., Fenton, W. A., Saibil, H. R. & Horwich, A. L. (1999) *Cell* **97,** 325–338.
19. Fenton, W. A. & Horwich, A. L. (2003) *Q. Rev. Biophys.* **36,** 229–256.
20. Braig, K., Otwinowski, Z., Hegde, R., Boisvert, D. C., Joachimiak, A., Horwich, A. L. & Sigler, P. B. (1994) *Nature* **371,** 578–586.
21. Fenton, W. A., Kashi, Y., Furtak, K. & Horwich, A. L. (1994) *Nature* **371,** 614–619.
22. Farr, G., Furtak, K., Rowland, M. C., Ranson, N. A., Saibil, H. R., Kirchhausen, T. & Horwich, A. L. (2000) *Cell* **100,** 561–573.
23. Zahn, R., Perrett, S. & Fersht, A. R. (1996) *J. Mol. Biol.* **261,** 43–61.
24. Zahn, R. & Plückthun, A. (1994) *J. Mol. Biol.* **242,** 165–174.
25. Walter, S., Lorimer, G. H. & Schmid, F. X. (1996) *Proc. Natl. Acad. Sci. USA* **93,** 9425–9430.
26. Ranson, N. A., Dunster, N. J., Burston, S. G. & Clarke, A. R. (1995) *J. Mol. Biol.* **250,** 581–586.
27. Ranson, N. A., Farr, G. W., Roseman, A. M., Gowen, B., Fenton, W. A., Horwich, A. L. & Saibil, H. R. (2001) *Cell* **107,** 869–879.
28. Landry, S. J., Zeilstra-Ryalls, J., Fayet, O., Georgopoulos, C. & Gierasch, L. M. (1993) *Nature* **364,** 255–258.
29. Xu, Z., Horwich, A. L. & Sigler, P. B. (1997) *Nature* **388,** 741–750.
30. Brinker, A., Pfeifer, G., Kerner, M. J., Naylor, D. J., Hartl, F. U. & Hayer-Hartl, M. (2001) *Cell* **107,** 223–233.
31. Goloubinoff, P., Christeller, J. T., Gatenby, A. A., and Lorimer, G. H. (1989) *Nature* **342,** 884–889.
32. Martin, J., Langer, T., Boteva, R., Schramel, A., Horwich, A. L. & Hartl, F. U. (1991) *Nature* **352,** 36–42.
33. Jackson, G. S., Staniforth, R. A., Halsall, D. J., Atkinson, T., Holbrook, J. J., Clarke, A. R. & Burston, S. G. (1993) *Biochemistry* **32,** 2554–2563.
34. Goldberg, M. S., Zhang, J., Sondek, S., Matthews, C. R., Fox, R. O., and Horwich, A. L. (1997) *Proc. Natl. Acad. Sci. USA* **94,** 1080–1085.
35. Lakowicz, J. R., Cherek, H., Gryczynski, I., Joshi, N. & Johnson, M. L. (1987) *Biophys. Chem.* **28,** 35–50.
36. Wu, P. & Brand, L. (1994) *Anal. Biochem.* **218,** 1–13.
37. Motojima, F. & Yoshida, M. (2003) *J. Biol. Chem.* **278,** 26648–26654.
38. Boisvert, D. C., Wang, J., Otwinowski, Z., Horwich, A. L. & Sigler, P. B. (1996) *Nat. Struct. Biol.* **3,** 170–177.
39. Farr, G. W., Fenton, W. A., Chaudhuri, T. K., Clare, D. K., Saibil, H. R. & Horwich, A. L. (2003) *EMBO J.* **22,** 3220–3230.
40. Ranson, N. A., Burston, S. G. & Clarke, A. R. (1997) *J. Mol. Biol.* **266,** 656–664.
41. Thorson, J. S., Chapman, E. & Schultz, P. G. (1995) *J. Am. Chem. Soc.* **117,** 9361–9362.
42. Miyazaki, T., Yoshimi, T., Furutsu, Y., Hongo, K., Mizobata, T., Kanemori, M. & Kawata, Y. (2002) *J. Biol. Chem.* **277,** 50621–50628.
43. Buckle, A. M., Zahn, R. & Fersht, A. R. (1997) *Proc. Natl. Acad. Sci. USA* **94,** 3571–3575.
44. Chen, L. & Sigler, P.B. (1999) *Cell* **99,** 757–768.
45. Jones, T.A., Zou, J.Y., Cowan, S.W. & Kjeldgaard, M. (1991) *Acta Crystallogr. A* **47,** 110–119.